A Time-Average Calculation For Bruce B Reactors Operating With Low-Void-Reactivity Fuel

C. Ngo-Trong

Atomic Energy of Canada Limited

Abstract

The computer code RFSP was used to perform a time-average calculation and related core characteristics calculations for Bruce B reactors, operating with either the current 37-element natural uranium (NU) fuel bundles or the CANFLEX®[1]-LVRF bundles.

It was found that the core flux/power distributions, fuel exit burnup and fuelling rate, when operating with Low-Void-Reactivity Fuel (LVRF), remain generally similar to those of the NU core. Where there are significant differences, they tend to enhance safety margins. The main difference is, by design, the coolant-density reactivity coefficient. Other beneficial differences are in the coolant-temperature, fuel-temperature and moderator-temperature reactivity coefficients. The smaller xenon transient at reactor shutdown from high power would provide an increase in xenon-override time.

1. INTRODUCTION

Bruce Power has undertaken a project, called the "New Fuel Project" [1], to replace 37-element natural uranium (NU) fuel, currently used in all Bruce B reactors, by CANFLEX Low-Void-Reactivity Fuel (LVRF) to restore robust safety margins and to return reactors to their rated power. It is expected that LVRF will provide the necessary enhancements in safety margins to operate the reactors at their design capacity [2].

The Bruce B Reference CANFLEX-LVRF bundle design is based on the CANFLEX Mark IV NU design [3]. It has NU fuel with dysprosium burnable poison in the central pin and slightly enriched uranium (SEU) fuel in the remaining fuel pins. A preliminary evaluation [2] showed that the selected design would achieve the same average fuel exit burnup as the current NU fuel, while reducing the full-core coolant-void reactivity by about 6 mk.

As part of the study of anticipated reactor performance in the New Fuel Project, AECL was commissioned by Bruce Power to set up a time-average model for reactor

[1] CANFLEX is a registered trademark of Atomic Energy of Canada Limited (AECL) and the Korea Atomic Energy Research Institute (KAERI).

operation with LVRF and related calculations of core characteristics. This paper gives a short summary of the findings.

2. TIME-AVERAGE CALCULATION OF REACTOR OPERATION WITH LVRF

The time-average calculation assumes that the reactor is already fully loaded with the new fuel and has operated with the new fuel for a sufficiently long time that the fuelling rate is practically constant with time (equilibrium fuelling). A time-average calculation uses nuclear cross sections for each fuel bundle, which provide cross-consistency among several calculated quantities, namely flux distribution, fuel-irradiation distribution, fuelling rate and scheme, and core reactivity. Required input data for a time-average calculation consists of irradiation-dependent lattice cross sections (fuel table), the refuelling scheme for each channel, the target fuel exit irradiation for each fuel channel (or each group of fuel channels), and the targeted channel power distribution. Time-average calculations have, over the years, been remarkably successful for CANDU®[2] reactor design and operation in the prediction of the averages (over time) of core flux and power distributions, fuel discharge burnup and fuelling rates. In addition, the core time-average model is also normally used to calculate static reactivity-device worths, static reactivity coefficients and the evolution of xenon transients.

2.1 Computer Codes and Sources of Input

The computer code RFSP, version REL_3-03HP [4], was used to perform the time-average calculation for Bruce B reactors operating at full power with LVRF bundles.

The reactor core was assumed to have been completely reconfigured before the core is fuelled with LVRF bundles. The reconfigured core differs from the existing core by having only 12 fuel bundles per channel (as opposed to 13) and by the use of fuelling-with-flow (FWF) refuelling, as compared to the current fuelling-against-flow (FAF) refuelling. In this configuration, the 12-bundle fuel string is not centred in the core, but is shifted about a half-bundle-length downstream. Part of the last bundle (bundle 12) is out of the core region, and there is some coolant in the channel upstream of the first bundle. The coolant upstream of the first bundle that is in the core region is modelled as a fictitious coolant “bundle” of the appropriate length.

The computer code WIMS-AECL [5], version 2.5d, with the 89-energy-group ENDF/B-VI library, modified to include the burnable dysprosium isotopes (version 1a1), was used to calculate lattice cross sections for LVRF bundles and cross sections for the fictitious coolant “bundles” (at the upstream end of the channel with coolant only, the

[2] CANDU® (CANada Deuterium Uranium) is a registered trademark of Atomic Energy of Canada Limited (AECL).

result of the reconfiguration to 12 bundles per channel). Table 1 gives the core conditions used in the calculation of the fuel tables.

Details of the core geometry, and coordinates and incremental cross sections of reactivity devices, were based on the Bruce B Reference Data Set (RDS) updated for LVRF. The update consists mainly in new incremental cross sections for adjusters, zone controllers, shutoff rods, control absorbers and their guide tubes that were recalculated for the new fuel with the computer code DRAGON [6].

The mesh array was revised, with new mesh lines to coincide with all lattice lines and the modelling of major reactivity devices in the x- and z-directions. The mesh spacing in the y-direction is set mostly to half lattice pitches, particularly near the top of the calandria, to enhance the precision of eventual *CERBERUS time-dependent simulations involving shutoff-rod drop into the core. The new numbers of mesh intervals in the core model are 50 x 54 x 39.

The refuelling scheme was revised to “fuelling with flow”. The normal push-through refuelling scheme was replaced by the corresponding generalized refuelling scheme to ensure that the water “bundle” remains at bundle position 1, counting from the flow-inlet end, at all times. The generalized refuelling scheme map is shown in Figure 1, where the schemes 28 and 24 correspond to the regular 8-bundle and 4-bundle shift schemes for the real fuel bundles; a positive number indicates coolant flow (and also fuelling direction in this case) from the reactor West face to the reactor East face; a negative number corresponds to coolant flow from East to West.

In Figure 1, the origin of the mesh-array coordinates is on the reactor West face, at the top left corner, 80 cm above the fuel channel row A, and 80 cm to the left of the fuel channel column 1. The x-axis is along the fuel channel rows. The y-axis is along the fuel channel columns. The z-axis is along the fuel channels, with positive direction from West to East.

The reference power distribution used in the time-average calculation is the RDS Reference derived from past operational history with SORO [Bruce B uses the computer code SORO for fuel management] time-averaged and normalized to full power. The SORO results were filtered to include only data above 88% full power (FP). This is shown in Figure 2.

2.2 Core Reactivity Bias

In principle, all time-average calculations should be done by selecting a fuel-channel exit-irradiation distribution in RFSP simulation, which gives, as close as possible, the reference power distribution and a k-eff of 1.0 (i.e., a core reactivity equal to 0 mk). This choice of core reactivity assumes that the RFSP-IST core model incorporates everything and its prediction of the core reactivity is error-free. In practice, the code results have uncertainties, which vary with core configuration.

For simplicity, it is assumed here that all core configurations pertaining to a normal or near normal operation of the reactor have the same simulated core reactivity error, or core reactivity bias.

The core reactivity bias was determined by performing a time-average calculation with the NU core model, with the exit irradiation distribution chosen to produce a time-average channel power distribution matching the RDS Reference, which is the SORO Time Averaged (SOROTA) power distribution, and with an average fuel exit burnup matching the corresponding average fuel exit burnup for Bruce B Unit 7 for the period selected. To reduce computation time without sacrificing accuracy, matching the channel-power distribution was taken to mean that the calculated channel powers were within 0.1% of the targets; similarly, matching the k-eff or core reactivity means getting a k-eff or a core reactivity within 0.01 mk of the target; matching a core-averaged fuel exit burnup means getting a core-averaged fuel exit burnup within 1 MWh/bundle of the target. Note that in this simulation to find the core reactivity bias, the reactor power was 90% FP, and 37-element NU fuel bundles were used.

Core conditions used to determine reactivity bias were based on typical operational values for Unit 7 for the period considered.

To match the SOROTA power distribution, individual channel exit irradiations were adjusted in an iterative procedure.

The calculated k-eff was 0.995941. The Bruce B RFSP-IST core reactivity bias is therefore –4.08 mk. Note that this bias is similar to the one observed for the domestic CANDU 6, which is about –3.5 mk [7].

The core reactivity bias, determined above for the NU core, will also be used without change for the LVRF core.

2.3 Time-Average Calculation with LVRF Bundles

The time-average calculation, at 100% FP, with LVRF bundles (and one fictitious coolant “bundle” at the channel inlet end) was done with the core model constructed as described in section 2.1. The Reference Power Distribution for the time-average calculation is SOROTAFP (SORO time-average at full power), shown in Figure 2. Individual fuel-channel exit irradiations were iteratively adjusted to produce a time-average channel power distribution matching SOROTAFP to within 0.1%. In parallel, the core-average exit irradiation was also adjusted to produce a core reactivity matching the core reactivity bias to within 0.01 mk.

RFSP-IST was programmed such that during the dwell time of each fuel channel, every fuel bundle in the channel has to move from one position to the other. The coolant bundle had to be discharged at each channel refuelling, and off-line adjustments of data were needed during the iteration process to take care of the discharge of the fictitious coolant bundles.

2.4 Results

Summary results of the time-average calculation with LVRF bundles are shown in Table 2. Those of the time-average calculation of section 2.2, with NU bundles, renormalized to 100% FP, are also shown in the same table for comparison.

As expected, the maximum channel powers are practically identical for the two cases (about 6540 kW), since the same RDS Reference (SOROTAFP) was used for power matching. The maximum bundle powers are also practically identical (about 756 kW).

The average thermal cell flux is lower in the LVRF core, 1.715×10^{14} n/cm^2.s, as compared to 1.863×10^{14} n/cm^2.s for the NU core. This is expected, since there are more fissile materials in the LVRF core, due to fuel enrichment, than in the NU core.

Correspondingly, the reactivity decay rate is about 25% higher in the LVRF core, -0.51 mk/FPD, as compared to –0.41 mk/FPD for the NU core.

The fuel exit burnup is about 6.5% higher for the LVRF bundles: 200 MWh/kgU for LVRF versus 188 MWh/kgU for NU fuel. However, the fuel feed rate is only marginally lower (3% lower) for LVRF. This is due to the fact that the current NU bundle has a slightly greater U mass per bundle than the LVRF bundle.

2.5 Time-Average-Equivalent Calculation

A time-average-equivalent model was also established for the LVRF core, with the explicit calculation of a fuel irradiation distribution, which would allow the use of the *SIMULATE module to calculate the core flux/power distributions. The core configuration is then both an instantaneous configuration (making it possible to simulate with the module *SIMULATE) and also an average over time of all instantaneous configurations of the same nominal conditions. The fuel irradiation was chosen so as to produce flux/power distributions calculated with *SIMULATE practically identical to those obtained in the time-average calculation. The resulting fuel-irradiation distribution is called a “time-average equivalent” model of the core.

Table 3 shows a comparison between the core power distribution from the time-average calculation for the LVRF core (discussed in sections 2.3 and 2.4) and that from the time-average-equivalent model, calculated with *SIMULATE. The two distributions are practically identical.

The time-average-equivalent model is more convenient to use than the time-average model, particularly with the possibility for history-based calculations with the *SIMULATE/SIMPLE-CELL-METHOD (SCM) [8] combination. The time-average-equivalent model for the Bruce B LVRF core will be used later for reactivity-coefficient and xenon-transient calculations.

3. STATIC REACTIVITY WORTHS

The reactivity-device worths are normally calculated with a time-average model. They are calculated here for the LVRF core, both with the time-average model and with the time-average-equivalent model. The results are shown in Table 4. Also shown in Table 4 are the device worths calculated for the NU core with the model explained in section 2.2.

As expected, the device worths are practically identical when calculated with the time-average or the time-average-equivalent model.

The device worths are systematically smaller in the LVRF core than in the NU core, consistent with a blacker fuel (LVRF has dysprosium in the central fuel element).

The effect of reduced SDS1 worth was inherently included in large-break loss-of-coolant-accident (LBLOCA) analysis with LVRF [2]. For the reactivity-control devices, control studies conclude that the small reductions in worths would have no significant impact on reactor controllability.

4. STATIC REACTIVITY COEFFICIENTS

The static reactivity coefficient is, by definition, the change in core reactivity induced by a unit change of a particular operating parameter value (coolant temperature, fuel temperature, moderator boron concentration, etc.), assuming that all other operating conditions and core configurations remain unchanged. It is an abstract concept and has often been calculated with a lattice cell code such as POWDERPUFS-V or WIMS.

Recent rapid advances in computing hardware and software make it possible to calculate these coefficients with ease and with very low computing costs, using more realistic 3-D, finite-core models. Here, these coefficients were calculated for the LVRF core with RFSP-IST, using the time-average-equivalent model of the reactor. All coefficients, except the fuel-temperature coefficient, were calculated using SCM. The fuel-temperature reactivity coefficient was calculated using WIMS fuel tables (fuel temperature is power dependent; average bundle fuel temperatures were internally calculated by the SCM module of RFSP; the core average fuel temperature was not readily available in a simulation with SCM).

The results are shown in Table 5. The same coefficients for the NU core, calculated with the same methodology, are also shown in Table 5 for comparison. The ranges of application for the given coefficients are included in the table.

The coolant-temperature reactivity coefficient (including the coolant-density effect) is 0.0266 mk/^{o}C in the LVRF core. It is significantly higher, at 0.0594 mk/^{o}C in the NU core. A lower coefficient is more desirable.

The coolant-density reactivity coefficient is –12.68 mk/g/cm^3 in the LVRF core, and is significantly higher for the NU core, at –18.55 mk/g/cm^3. The difference reflects the reduction in void reactivity with LVRF bundles.

The moderator-temperature reactivity coefficient (including the density effect) is -0.0165 mk/^{o}C for the LVRF core and is 0.0451 mk/^{o}C for the NU core. A negative coefficient improves safety margins.

The coolant-purity reactivity coefficient is practically the same in the LVRF and NU cores, about 0.7 mk/at%.

The moderator-purity reactivity coefficient, the moderator-boron reactivity coefficient and the moderator-gadolinium reactivity coefficient are about 10% lower in the LVRF core than in the NU core.

The fuel-temperature reactivity coefficient at full power is –0.0037 mk/^{o}C for the LVRF core. It is very close to zero, at –0.0015 mk/^{o}C, for the NU core.

The fuel-temperature coefficient at hot shutdown is –0.0084 mk/^{o}C for the LVRF core. It is again close to zero, at –0.0021 mk/^{o}C, for the NU core. A more negative coefficient improves safety margins.

Note that all the reactivity coefficient values mentioned above are only for limited ranges of application, which are specified in Table 5.

5. XENON TRANSIENTS

Xenon transients refer to the changes to the reactivity associated with the core xenon load over time, initiated by a reactor power level change. Earlier physics design calculations for CANDU reactors provided results for xenon transients only (excluding other saturating fission products), to maintain computing cost at reasonable level.

Recent rapid advances in computing hardware and software make it possible to calculate more accurately, with ease and with very low computing costs, the core reactivity transients following a change in reactor power level, by including also other non-negligible saturating fission products and neutron-reaction products. More specifically, the following nuclides were included in this study when calculating the core-reactivity transients following a reactor power level change: ^{135}Xe, ^{149}Sm, ^{151}Sm, ^{155}Eu, ^{113}Cd, ^{105}Rh, ^{157}Gd and ^{239}Np. The results will be more realistic and useful to the operation. The title of this section (Xenon Transients) is therefore somewhat of a misnomer. It is kept here for tradition, and also because the term is familiar to most readers.

Figure 3 shows the core reactivity transients after shutdown from various power levels (100%, 80%, 60%, 40% and 20% of full power). The calculations were done with all adjuster rods (ADJ) in core, all control absorbers (CA) and shutoff rods (SOR) out of core, and all zone controllers (ZCR) at 40% fill.

Saturating-fission-product loads are highest at about 10 h after shutdown for shutdowns from 100% FP and 80% FP, at about 9 h after shutdown for shutdowns from 60% FP and 40% FP, and at about 7 h after shutdown for a shutdown from 20% FP.

Saturating-fission-product loads return to the same values as before shutdown after about 40 h, 38 h, 34 h, 29 h and 20 h for shutdowns from 100% FP, 80% FP, 60% FP, 40% FP and 20% FP, respectively.

The core reactivity transient after shutdown from 100% FP was also calculated for the NU core. Figure 4 shows both curves for the LVRF and the NU cores for comparison.

Saturating-fission-product peak loads are significantly lower in an LVRF-fuelled core than in a NU-fuelled core. For a shutdown from 100% FP, the peak load is about -77 mk for the LVRF core and about –103 mk for the NU core. This change is due mainly to a reduction in the ^{135}I / ^{135}Xe concentration ratio with fuel enrichment. A smaller xenon transient at reactor shutdown from high power would result in an increase in xenon-override time.

Figure 5 shows the core reactivity transients following power reductions from full power to 60% FP in 364 s, to 30% FP in 318 s, to 20% FP in 727 s, to 11% FP in 162 s and to 2% FP in 891 s. The selected end-powers and rates of power change were taken from Reference [9].

As in the above case of shutdown transients, the RFSP calculations for these power-reduction cases were also done with all the adjusters in the core, all control absorbers and shutoff rods out of core, and all zone control units at 40% fill.

The time 0 in Figure 5 is when the reactor first reaches the end-power.

For setbacks to end-power 20% FP or higher, the fission product reactivity transients show some oscillations after the saturating fission product loads return to their equilibrium values before the setbacks. This behaviour, also observed in previous calculations for Bruce A reactors with the 37-element NU fuel bundles, is the result of having all saturating fission products and ^{239}Np included in the reactivity transient calculations, but is not seen in the corresponding xenon-only transients.

Figure 6 shows the core reactivity transients following start-up to various steady-state power levels (20%, 40%, 60%, 80% and 100% of full power), following a very long shutdown. The power increase was assumed to be instantaneous. The reactor is at power at time 0 in Figure 6. Reactivity-device positions are the same as in the previous transients.

6. CONCLUSION

A time-average calculation and related core characteristic calculations were performed for the Bruce B reactors, operating at equilibrium fuelling conditions with CANFLEX-LVRF bundles, using advanced computer codes and core modelling methods.

It has been shown that the core behaviour remains very similar to that of the NU core. Where there are significant differences, they tend to provide for improved safety margins. The main difference is, by design, the coolant-void reactivity (or, equivalently,

the coolant-density reactivity coefficient). Other beneficial differences are in the coolant-temperature, fuel-temperature and moderator-temperature reactivity coefficients. The smaller xenon transient at reactor shutdown from high power would provide an increase in xenon-override time.

ACKNOWLEDGEMENTS

All calculations presented here for the Bruce B LVRF core were performed for Bruce Power by AECL through the NSS/AECL Consortium.

The author wishes to thank Bruce Power and the Consortium for permission to use these results for this paper.

REFERENCES

1) M. LISKA and D. MCARTHUR, “Bruce Power New Fuel Project, CANFLEX-LVRF Project Overview”, in Proceedings of the 25th Annual Conference of the Canadian Nuclear Society, Toronto, Ontario, Canada, June 6-9 (2004).
2) G.H. ARCHINOFF, O. NAINER, H.H. WONG, D.R. NOVOG and T.V. TRAN, “Safety Benefits of Low Void Reactivity Fuel in Bruce B”, in Proceedings of the 25th Annual Conference of the Canadian Nuclear Society, Toronto, Ontario, Canada, June 6-9 (2004).
3) K.S. SIM, M.R. FLOYD, S.J. PALLECK, F.J. DORIA and J.H. LAU, “CANFLEX LVRF Fuel Performance Qualification”, in Proceedings of the 25th Annual Conference of the Canadian Nuclear Society, Toronto, Ontario, Canada, June 6-9 (2004).
4) B. ROUBEN, “RFSP-IST, The Industry Standard Tool Computer Program for CANDU Reactor Core Design and Analysis”, in Proceedings of the 13th Pacific Basin Nuclear Conference, Shenzhen, China, October 21-25 (2002).
5) D. IRISH and S.R. DOUGLAS, “Validation of WIMS-IST”, in Proceedings of 23rd Annual Conference of the Canadian Nuclear Society, Toronto, June 2-5 (2002).
6) G. MARLEAU, A. HEBERT, and R. ROY, “A User’s Guide for DRAGON Version DRAGON_980911 Release 3.03”, Technical Report IGE-174 Rev. 4, Institut de Genie nucleaire, Departement de genie mecanique, Ecole Polytechnique de Montreal, Septembre (1998).
7) B. ARSENAULT, J.V. DONNELLY, and D.A. JENKINS, "History-Based Calculations Using WIMS-AECL in RFSP", 20th Nuclear Simulation Symposium Niagara-on-the-Lake September 7-9 (1997).
8) J. V. DONNELLY, “Development of a Simple-Cell Model for Performing History-Based RFSP Simulations with WIMS-AECL”, in Proceedings of the International

Conference on the Physics of Nuclear Science and Technology, Long Island, NY, October (1998).

9) BRUCE B SAFETY REPORT, Chapter 2, November (1999).

TABLE 1. CORE CONDITIONS USED IN WIMS CALCULATIONS OF 2-GROUP FUEL TABLES

Parameter	LVRF Reference Design	RDS 37-ELMT NU FUEL	Unit 7 2000/01/01 to 2001/09/14
Reactor Power (%FP)	100	100	90
Coolant Temperature (degree C)	284	284.98	280
Coolant Density (g/cc)	0.822	0.8212	0.832
Coolant Purity (at% D2O)	98.882	98.8	98.882
Fuel Temperature (degree C)	674	748.57	697.23
Moderator Temperature (degree C)	68.2	64.0	68.2
Moderator Density (g/cc)	1.0858	1.08811	1.0858
Moderator Purity (at% D2O)	99.9453	99.0	99.9453
Moderator Boron Concentration (ppm)	0.029	0.029	0.029
Moderator Gadolinium Concentration (ppm)	0.0	0.0	0.0
Average Pressure Tube Creep (%)	3.0	1.5	1.5

TABLE 2. COMPARISON IN OPERATING CHARACTERISTICS BETWEEN A 37-ELEMENT-NATURAL-URANIUM-FUELLED CORE AND A CANFLEX-LVRF-FUELLED CORE

Parameter	37-element NU fuel*	Reference Design LVRF
Maximum Channel Power (kW)	6539	6537
Maximum Bundle Power (kW)	757.2	755.5
Average Thermal Cell Flux (n/cm^2.s)	1.863E+14	1.715E+14
Reactivity Decay Rate (mk/FPD)	-0.4129	-0.5102
Average Fuel Exit Burnup (MWh/bundle)	3617	3732
Average Fuel Exit Burnup (MWh/kgU)	188.3	200.4
Feed Rate (channels/FPD)	4.39	4.25
Feed Rate (bundles/FPD)	18.80	18.22

*renormalized to 100% FP

TABLE 3. ANALYSIS OF RATIOS OF SIMULATE POWERS OVER TIME-AVERAGE POWERS

Ratios	Number of Channels or Bundles	Average	Standard Deviation	Maximum	Minimum	RMS
Channel Powers in Zone_8*	100	1.009879	0.004887	1.017818	0.9994	1.009891
Channel Powers in Zone_4**	380	0.99856	0.003776	1.009752	0.993363	0.998567
Channel Powers in Whole Core	480	1.000918	0.006195	1.017818	0.993363	1.000937
Bundle Powers	5760	0.999323	0.007052	1.022905	0.98726	0.999348

* Zone_8 includes all 8-bundle shift channels
**Zone _4 includes all 4-bundle shift channels

TABLE 4. DEVICE STATIC REACTIVITY WORTHS

Device	Calculated Device Static Reactivity Worth (mk) for a LVRF Core		Device Worths for a NU Core
	*TIME-AVER	*SIMULATE	
ZCR fill change from 0% to 100%	-6.45	-6.45	-6.90
All adjusters withdrawn	17.35	17.19	19.35
All control absorbers inserted	-8.72	-8.7	-9.47
All shutoff rods inserted	-65.32	-64.89	-70.30

TABLE 5. BRUCE B LVRF CORE REACTIVITY COEFFICIENTS

Parameter	Range of application	Value	
		LVRF-fuelled core	NU-fuelled core
Coolant Temperature Reactivity Coefficient (incl. Density)	+/- 25 °C about 284 °C	0.0266 mk/°C	0.0594 mk/°C
Coolant Density Reactivity Coefficient	+/- 0.1 g/cc about 0.82048 g/cc	-12.68 mk/g/cc	-18.55 mk/g/cc
Moderator Temperature Reactivity Coefficient (incl. Density)	+/- 12 °C about 68.2 °C	-0.0165 mk/°C	0.0451 mk/°C
Coolant Purity Reactivity Coefficient	+/- 0.5 at% about 98.882 at%	0.73 mk/at%	0.71 mk/at%
Moderator Purity Reactivity Coefficient	+/- 0.05 at% about 99.9453 at%	28.36 mk/at%	31.19 mk/at%
Moderator Boron Reactivity Coefficient	0 to 0.5 ppm	-6.96 mk/ppm	-7.46 mk/ppm
Moderator Gadolinium Reactivity Coefficient	0 to 0.1 ppm	-23.95 mk/ppm	-25.69 mk/ppm
Fuel Temperature Reactivity Coefficient at Full Power	+/- 100 °C about 674 °C for LVRF; +/- 100 °C about 750 °C for NU	-0.0037 mk/°C	-0.0015* mk/°C
Fuel Temperature Reactivity Coefficient at Hot Shutdown	264 °C to 364 °C	-0.0084 mk/°C	-0.0021 mk/°C

*Calculated with WIMS only

	1	2	3	4	5	6	7	8	9	10	11	12	13	14	15	16	17	18	19	20	21	22	23	24
A								-28	28	-28	28	-28	28	-28	28	-28	28							
B						28	-28	28	-28	28	-28	24	-24	28	-28	28	-28	28	-28					
C					28	-28	24	-24	24	-24	24	-24	24	-24	24	-24	24	-24	28	-28				
D				28	-28	24	-24	24	-24	24	-24	24	-24	24	-24	24	-24	24	-24	28	-28			
E			28	-28	24	-24	24	-24	24	-24	24	-24	24	-24	24	-24	24	-24	24	-24	28	-28		
F		28	-28	24	-24	24	-24	24	-24	24	-24	24	-24	24	-24	24	-24	24	-24	24	-24	28	-28	
G		-28	24	-24	24	-24	24	-24	24	-24	24	-24	24	-24	24	-24	24	-24	24	-24	24	-24	28	
H		28	-24	24	-24	24	-24	24	-24	24	-24	24	-24	24	-24	24	-24	24	-24	24	-24	24	-28	
J	28	-28	24	-24	24	-24	24	-24	24	-24	24	-24	24	-24	24	-24	24	-24	24	-24	24	-24	28	-28
K	-28	24	-24	24	-24	24	-24	24	-24	24	-24	24	-24	24	-24	24	-24	24	-24	24	-24	24	-24	28
L	28	-24	24	-24	24	-24	24	-24	24	-24	24	-24	24	-24	24	-24	24	-24	24	-24	24	-24	24	-28
M	-24	24	-24	24	-24	24	-24	24	-24	24	-24	24	-24	24	-24	24	-24	24	-24	24	-24	24	-24	24
N	24	-24	24	-24	24	-24	24	-24	24	-24	24	-24	24	-24	24	-24	24	-24	24	-24	24	-24	24	-24
O	-28	24	-24	24	-24	24	-24	24	-24	24	-24	24	-24	24	-24	24	-24	24	-24	24	-24	24	-24	28
P	28	-24	24	-24	24	-24	24	-24	24	-24	24	-24	24	-24	24	-24	24	-24	24	-24	24	-24	24	-28
Q	-28	28	-24	24	-24	24	-24	24	-24	24	-24	24	-24	24	-24	24	-24	24	-24	24	-24	24	-28	28
R		-28	24	-24	24	-24	24	-24	24	-24	24	-24	24	-24	24	-24	24	-24	24	-24	24	-24	28	
S		28	-24	24	-24	24	-24	24	-24	24	-24	24	-24	24	-24	24	-24	24	-24	24	-24	24	-28	
T		-28	28	-24	24	-24	24	-24	24	-24	24	-24	24	-24	24	-24	24	-24	24	-24	24	-28	28	
U			-28	28	-24	24	-24	24	-24	24	-24	24	-24	24	-24	24	-24	24	-24	24	-28	28		
V				-28	28	-24	24	-24	24	-24	24	-24	24	-24	24	-24	24	-24	24	-28	28			
W					-28	28	-24	24	-24	24	-24	24	-24	24	-24	24	-24	24	-28	28				
X						-28	28	-28	28	-28	28	-24	24	-28	28	-28	28	-28	28					
Y								28	-28	28	-28	28	-28	28	-28	28	-28							

FIGURE 1: GENERALIZED FUELLING SCHEMES USED IN THE BRUCE B TIME-AVERAGE MODEL WITH LVRF AND COOLANT BUNDLES

	1	2	3	4	5	6	7	8	9	10	11	12	13	14	15	16	17	18	19	20	21	22	23	24
A								3174	3475	3703	3891	4012	3921	3889	3709	3493	3193							
B						3298	3850	4281	4564	4722	4864	5065	5067	4889	4743	4595	4305	3911	3319					
C					3710	4303	4923	5321	5552	5726	5824	5787	5863	5895	5764	5594	5332	4961	4327	3745				
D				3743	4441	5212	5700	5927	6108	6210	6302	6290	6323	6314	6255	6128	5936	5676	5242	4499	3859			
E			3654	4392	5246	5824	6155	6324	6312	6344	6403	6383	6392	6434	6343	6337	6295	6118	5811	5312	4469	3689		
F		3195	4057	5134	5790	6202	6335	6378	6405	6416	6416	6350	6352	6428	6453	6416	6388	6242	6155	5768	5164	4152	3181	
G		3669	4754	5603	6036	6277	6357	6445	6455	6457	6401	6203	6273	6444	6487	6481	6448	6350	6281	6075	5580	4785	3646	
H		4036	5187	5893	6170	6235	6323	6481	6494	6466	6458	6272	6300	6461	6498	6511	6473	6342	6246	6145	5907	5176	4179	
J	3349	4401	5482	6052	6213	6205	6256	6450	6494	6522	6486	6423	6432	6481	6530	6496	6427	6266	6172	6217	6045	5456	4407	3333
K	3591	4769	5635	6190	6260	6184	6210	6384	6455	6520	6518	6500	6480	6460	6501	6465	6362	6180	6210	6293	6211	5660	4754	3570
L	3762	4915	5762	6227	6306	6224	6253	6442	6472	6474	6522	6512	6521	6481	6501	6454	6388	6250	6197	6285	6311	5815	4897	3709
M	3896	4993	5810	6272	6337	6351	6430	6437	6458	6443	6472	6473	6471	6476	6452	6438	6463	6422	6368	6364	6377	5888	4966	3896
N	3932	5017	5835	6304	6378	6463	6492	6501	6466	6462	6432	6427	6365	6431	6383	6416	6475	6487	6434	6411	6314	5902	5010	3937
O	3725	4925	5825	6315	6423	6476	6425	6495	6473	6447	6410	6310	6303	6415	6460	6453	6491	6497	6462	6438	6325	5838	4935	3781
P	3613	4817	5716	6257	6361	6484	6496	6497	6483	6434	6427	6306	6297	6453	6472	6472	6494	6501	6426	6414	6317	5727	4821	3611
Q	3383	4456	5517	6150	6402	6430	6444	6538	6535	6471	6446	6478	6453	6483	6474	6516	6533	6447	6411	6342	6220	5608	4464	3365
R		4241	5255	6000	6258	6358	6390	6498	6511	6502	6498	6491	6495	6515	6465	6492	6504	6432	6397	6254	6005	5284	4239	
S		3717	4889	5670	6126	6268	6306	6404	6463	6477	6494	6505	6504	6488	6478	6425	6406	6258	6278	6102	5640	4904	3710	
T		3199	4173	5154	5768	6007	6123	6384	6445	6443	6442	6415	6398	6430	6405	6403	6348	6102	6008	5744	5132	4171	3216	
U			3672	4420	5201	5624	5973	6316	6348	6385	6324	6233	6212	6288	6320	6343	6267	5934	5587	5174	4397	3666		
V				3767	4375	5092	5585	5975	6126	6184	6141	6005	5998	6150	6168	6130	5935	5561	5042	4332	3733			
W					3558	4136	4780	5218	5546	5640	5666	5526	5515	5644	5608	5497	5237	4752	4094	3430				
X						3049	3661	4110	4429	4571	4680	4815	4809	4667	4549	4403	4093	3642	3022					
Y								2914	3245	3473	3651	3751	3666	3632	3450	3226	2899							

FIGURE 2: THE REFERENCE CHANNEL POWER DISTRIBUTION SOROTAFP IN KW

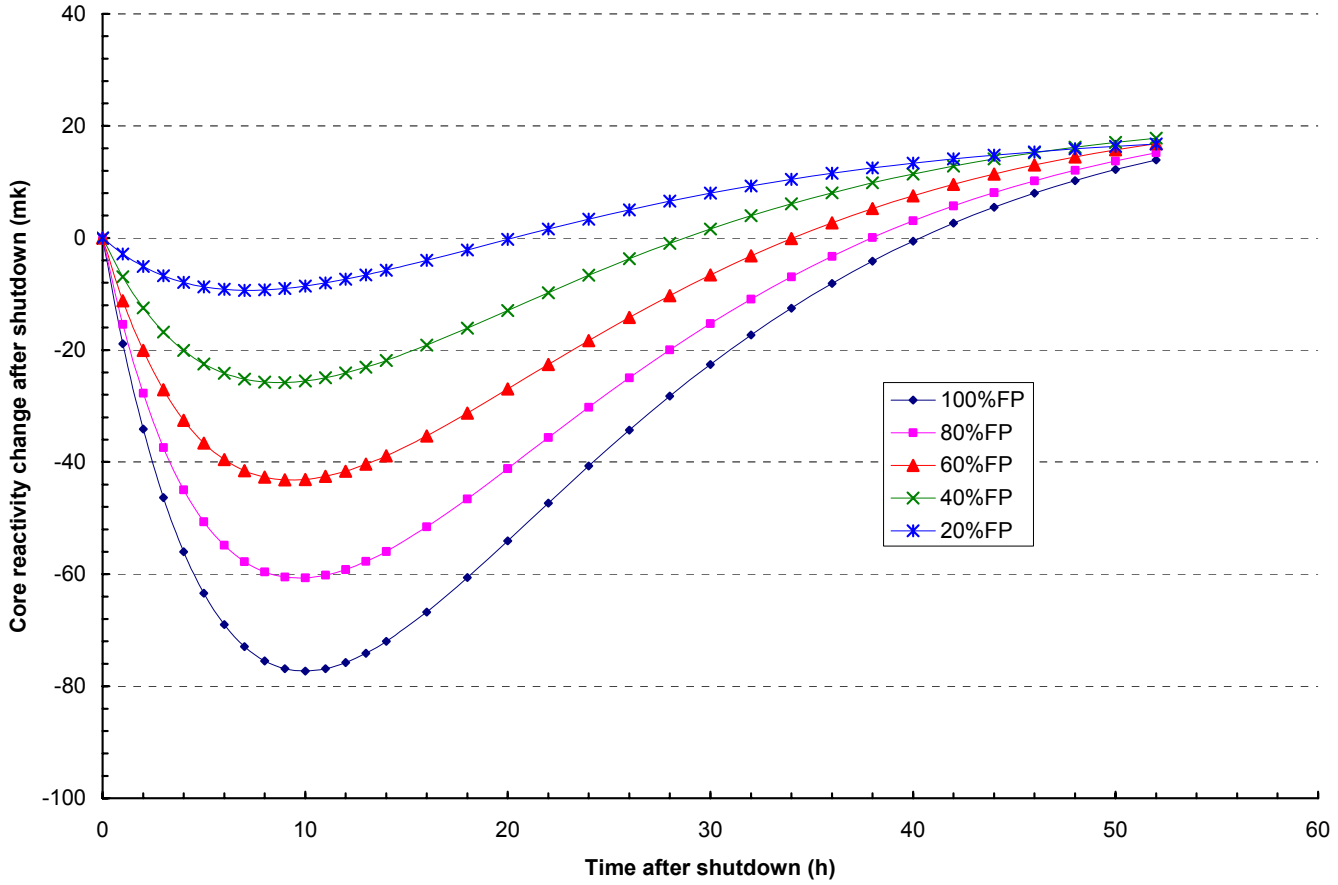

FIGURE 3: SHUTDOWN FROM VARIOUS POWER LEVELS

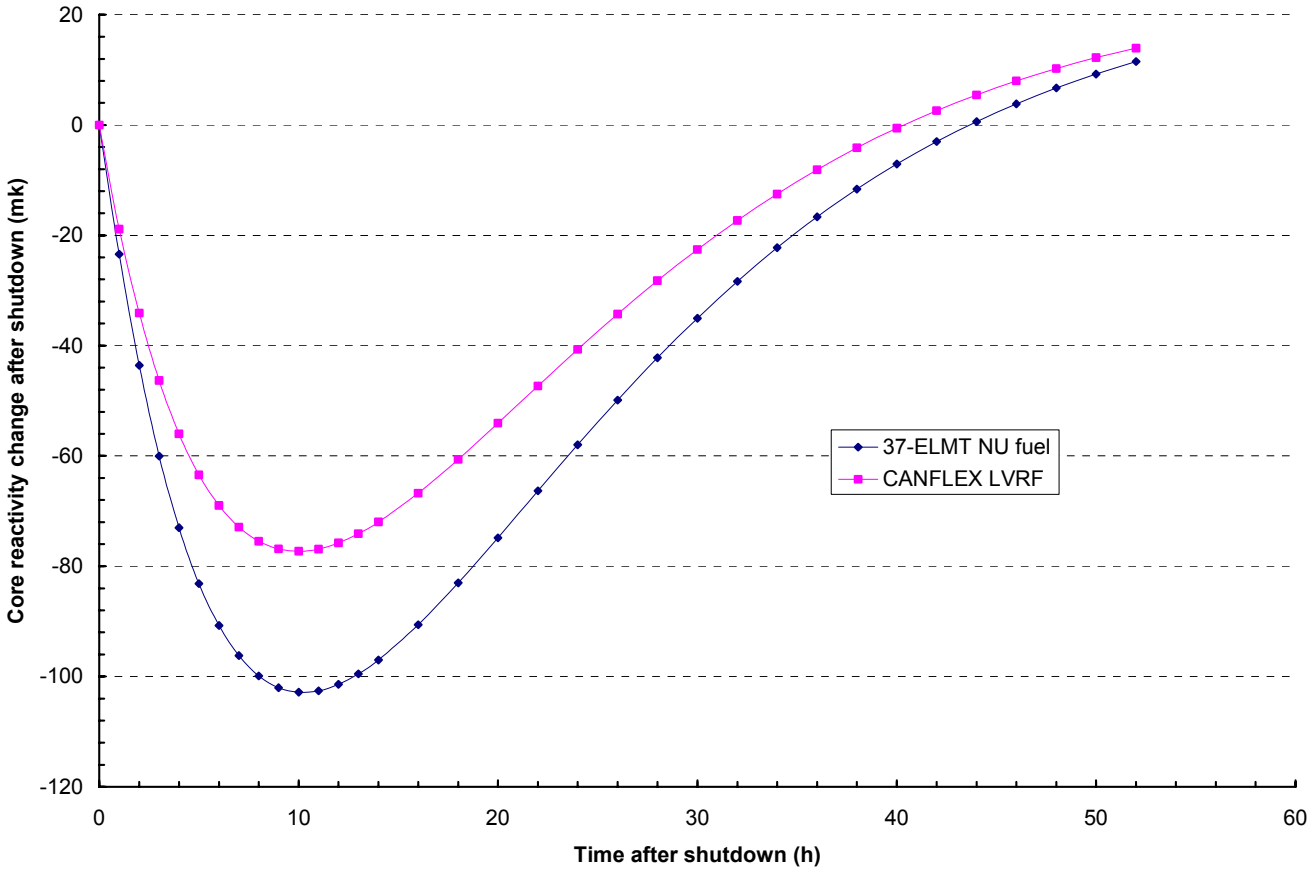

FIGURE 4: SHUTDOWN FROM 100% FP

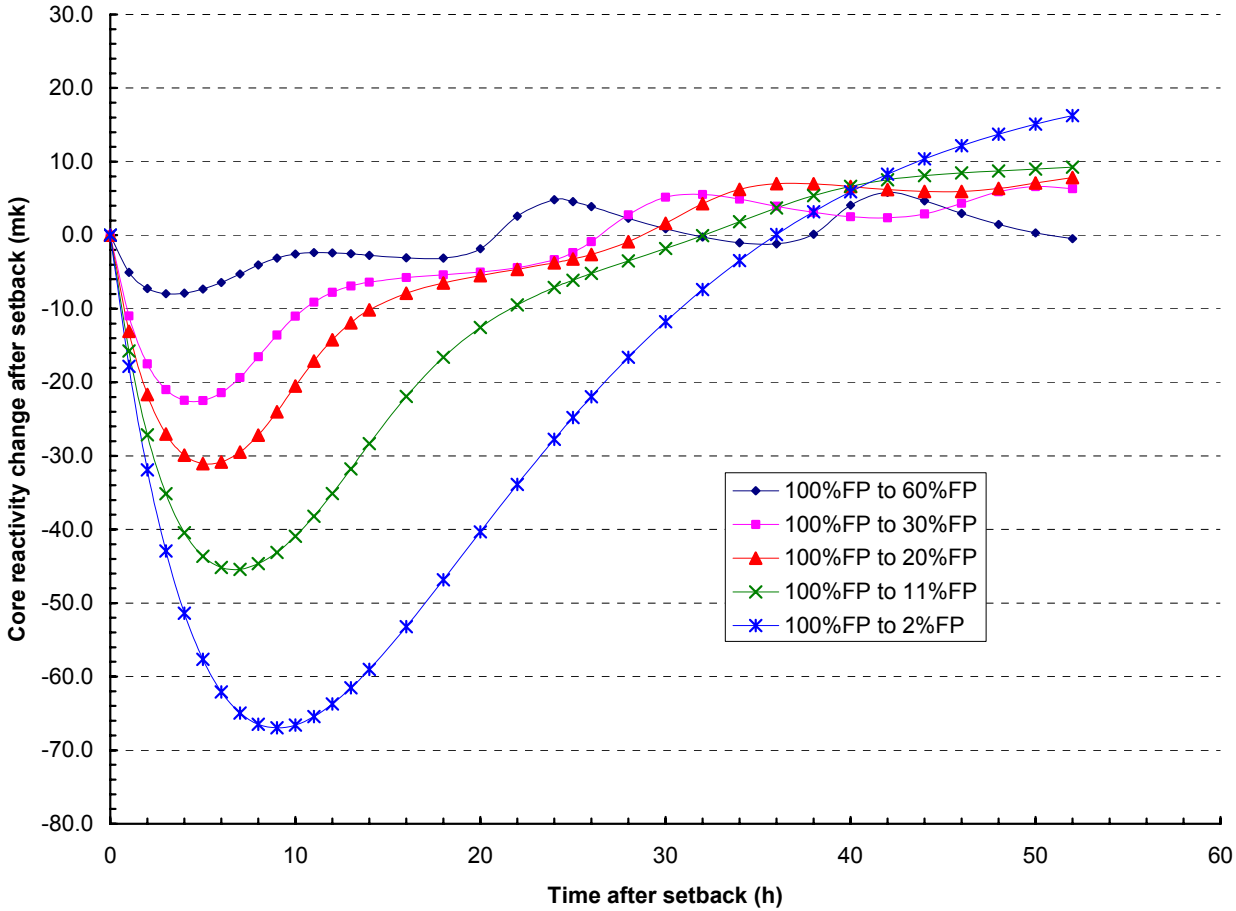

FIGURE 5: SETBACK FROM FULL POWER

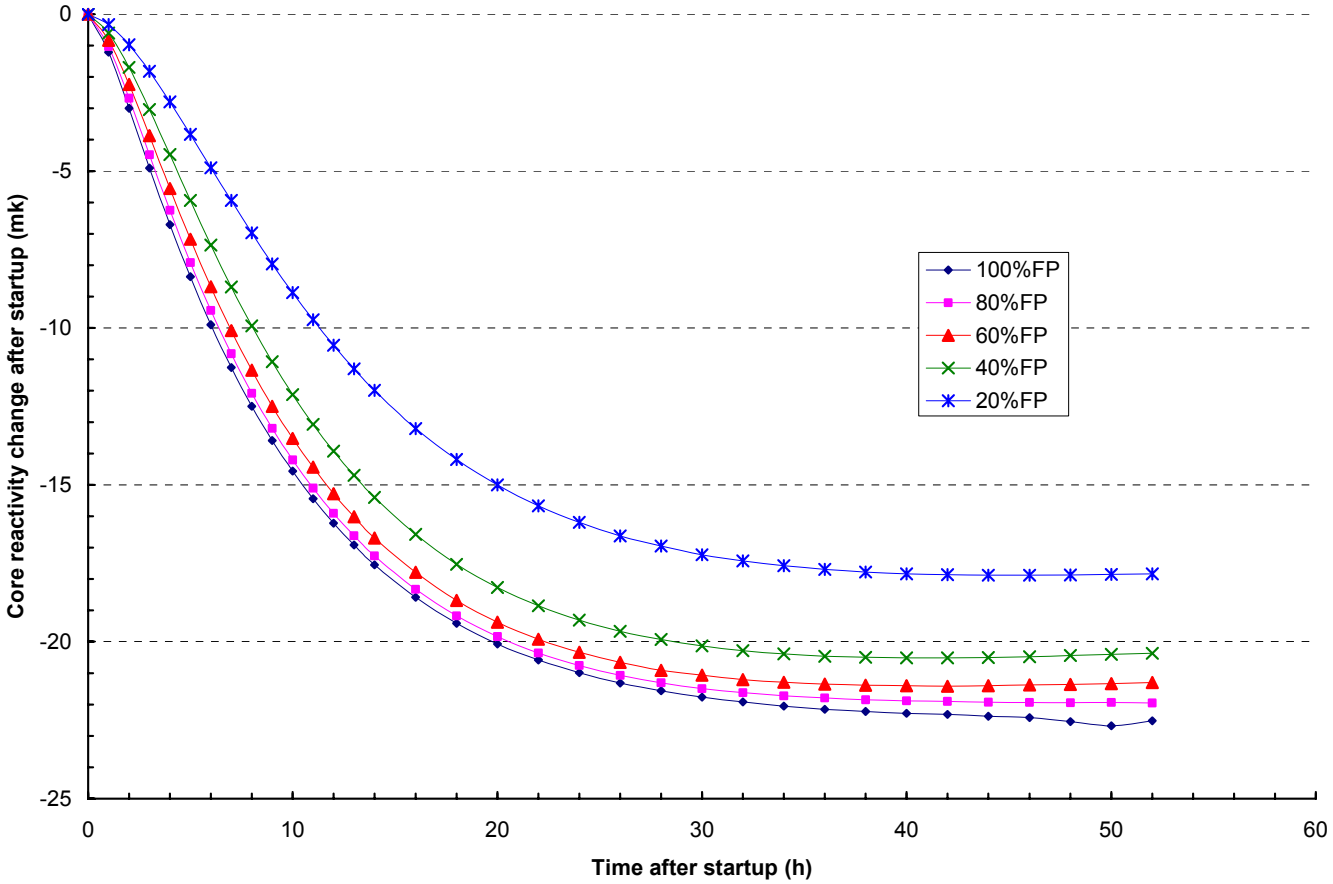

FIGURE 6: START-UP AFTER A VERY LONG SHUTDOWN